

# Experimental Study of the Sequel Events after Drop Impacting a Small Target

Merav Arogeti<sup>\*1</sup>, Eran Sher<sup>2</sup>, Tali Bar-Kohany<sup>3,4</sup>

<sup>1</sup>Mechanical Engineering, Sami Shamoon College of Engineering, Beer Sheva, Israel

<sup>2</sup>Faculty of Aerospace Engineering, Technion - Israel Institute of Technology, Haifa, Israel

<sup>3</sup>Mechanical Engineering Department, NRCN, Israel

<sup>4</sup>School of Mechanical Engineering, Tel-Aviv University, Tel-Aviv, Israel

\*Corresponding author: [meravar@sce.ac.il](mailto:meravar@sce.ac.il)

## Abstract

The after-events that follow a drop impact on a solid surface depend on the drop's initial conditions, drop properties, and the characteristics of the impactor surface. The limited impact surface area of the target generates unique three-dimensional responses that are different from those occurring when a drop impacts an infinite flat surface. The initial drop velocity has a significant influence on the outcome. High-velocity impact generates prompt splash; mild velocity generates receding corona breakup, and deposition is obtained for low velocity. Those known outcomes for an infinite flat surface were redefined here and characterized according to the particular influence of the small target dimensions. The receding breakup in small targets occurs while the drop is completely in the air, while maintaining its radial position, unlike the receding corona breakup or prompt splash breakup on large, plane surfaces. Moreover, it was deduced that as the target diameter increases, the likelihood of breakup or splash increases.

## Keywords

Small target, Drop impact, After-event

## Introduction

Drop impact phenomenon studies discuss the different parameters between cases, the drop properties, initial conditions, and the interface with a specific impact surface. A better understanding of the response after the impact enables controlling the liquid flow, whether it is required for aerosols, printing, or even drainage problems.

Rein, [1] indicates three impact results bouncing, spreading, and splashing, and [2] extended and detailed the division to six different drop impact outcomes on solid surfaces. Deposition, prompt splash, corona splash, receding breakup, partial and complete rebound, each outcome results from a different combination of the impact characteristics, and any change in the impact condition can change the outcome.

The surface target geometry controls the outcomes' shape and intensity. Increasing the curvature of sphere targets promotes splashing [3] and horizontal target surface compared to tilted [4] the splashing level response to the amount of kinetic energy transformed into the spreading process.

The after-event response of a drop impact on a small target differs from impact responses on a large horizontal surface. The small target does not provide enough surface for the drop to spread along the surface. Therefore, the drop continues the spread to the free air and is described as ejection [5]. In addition, small targets with polygons profile control the after-event spread directions [6]. The ejected lamella response reminds liquid lamella on

superhydrophobic surfaces. The absence of a surface under the lamella can be considered a hydrophobic contact angle [7].

The limited impact surface area of the target generates unique three-dimensional responses that are different from those occurring when a drop impacts a large flat surface [2].

A portion of the drop volume maintains the drop's falling velocity if the drop diameter is larger than the target diameter [8]. Therefore, the responses to the impact require a specific definition to address the boundary effects.

### Material and Methods

Freefall spherical water drops from different heights impact the horizontal top of cylindrical targets of different sizes. We recorded the impact and the after-event at 1000 frames per second, using two cameras for front and side views to confirm the drop and target alignment.

### Results and Discussion

We observed different impact after-events and defined the events following the definitions for drops impacts on a plane surface, referencing the specific forces acting on the drop after hitting the small target. The events are deposition, prompt splash, and in between the receding breakup.

**The deposition-** the drop deforms as one unit during the entire impact after-event [2]. Contrary to the big surface, the small target cannot stop the entire vertical velocity (momentum) and, therefore, the drop maintains part of its initial vertical inertial force. The deposition definition remains the same, with no breakup, but instead of flat spreading and receding to equilibrium, the drop spreads around the small target as a dish and recedes. The drop continues the fall along the target (see Figure 1). The spreading dish shape and the downward drop velocity varies according to the ratio of the target-to-drop diameter [8]

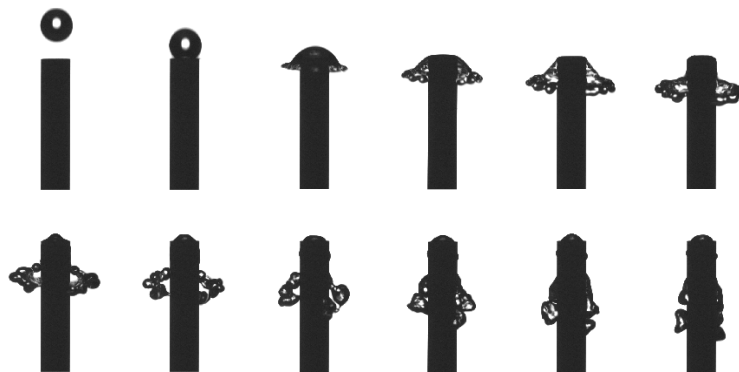


**Figure 1.** Drop impacts a small target- deposition sequence outcome.  $D_0 = 2.7[mm]$ ,  $D_t = 2.4[mm]$ ,  $v_0 = 1.65[m/s]$ , time sequences 1[msec]

**Prompt splash-** The drop splits into secondary drop with radial velocity, and the drops detached during the spreading phase, as shown in Figure 2. The majority of the drop fragments develops after the impact during the spreading phase. The fragmentation three stages [9] are almost similar to all atomization processes; the initial drop flattens to a pancake shape, most of the volume accumulates at the surrounding rim, the rim corrugates with fingers, and different sizes of drop detach from the fingers. The fingers formation on a small target as for a big surface, are followed by subsequent drops creation development with the lamella growing. The fingers around the rim behave like tiny jets that split into smaller drop due to Savart-Plateau-Rayleigh instability [5].

After the fingering, the surface tension minimizes the energy by gathering the liquid. The surface tension acts along the finger's length towards the finger's central axis. The directional surface forces with the radial velocity narrow the finger and create necks along the finger, ripping the liquid and creating splashed secondary drops with radial outward velocity. The splashed drop stabilize after the spread surrounding rim begins the receding phase [10]. Increased falling velocity can be a compensation for the lack of impact area and can enable prompt splash. The independent motion of the secondary drop consists of radial and vertical momentum.

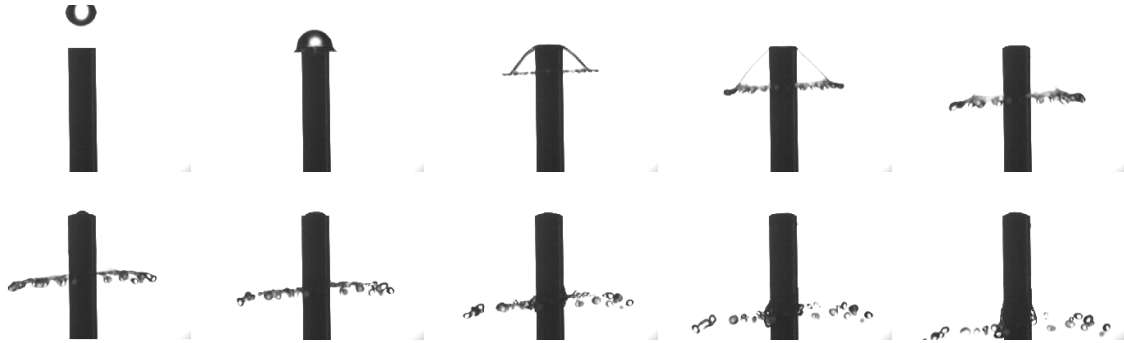


**Figure 2** Drop impacts a small target- Prompt splash after-event, the secondary drop continues to move away radially.  $D_0 = 2.7[mm]$ ,  $D_t = 2.4[mm]$ ,  $v_0 = 2.75[m/s]$ , time sequences 1[msec]

Development of a prompt splash requires high radial inertial force. The impact area controls the drop's initial energy transform to kinetic energy with radial velocity. A high drop-to-target diameters ratio that characterizes a small target allows a more significant portion of the volume to spread and eject radially. The influence of this high ratio is balanced by the liquid boundary layer, which reduces the velocity. We compare the spreading curve of three different drop-to-target diameters ratios see Figure 3. The after-events in this figure are deposition for the small and the big targets and prompt splash for the medium, 3 mm target, with secondary drop that continued the spread.

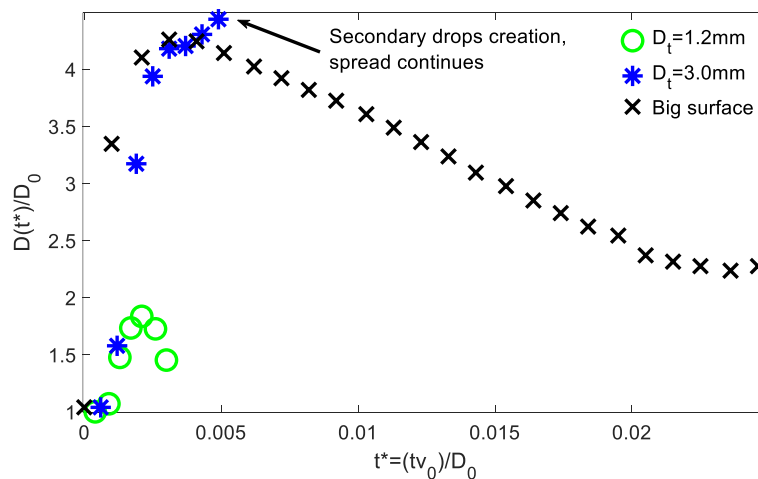


**Figure 3** After-event, diameter spread for three different impact target dimensions with similar drop and initial conditions.  $D_0 = 2.7[mm]$ ,  $v_0 = 2.80 [m/s]$

**Receding corona breakup-** This intermediate after-event generates secondary drops, without any farther radial spreading. The horizontal drop spread reaches the end of the target and continues the radial motion in the air with an inclination downward like an inverted bowl. The surrounding rim concentrates most of the drop volume [5] [11]. The acting forces on the drop determine the rim surface smoothness level, meaning whether finger formation initiates or not.

The energy of mild impact velocity is high enough to destabilize the drop and the rim. Contraction forces along the fingers [11] leading to the rim excitation and enable secondary drops between the spreading and receding phases. Receding breakup outcome was observed also for the impact of a drop on a plane surface. For that case it is a pure wetting phenomenon for a plane surface that stems from the decrease of the dynamic contact angle [2]. The receding corona breakup is separated from the plane surface impact due to the surface absence. The breakup occurs while the drop is completely in the free air without any surface friction forces. This breakup shape resembles a corona; the peripheral surrounding secondary drops are like the diamonds at the crown top, however it is not the known splash corona for the large surface due to the distinct difference in the formation stage, which leads to a corona shape without upward velocity. The exact values of such mean velocities depend on the drop-to-target diameter ratio and should be further investigated.

Once the new drops are formed, they begin their free fall downwards; the drop approximately maintains its horizontal position around the target from the moment of formation, as shown in Figure 4. This outcome agrees with the large surface receding breakup, for the secondary drops retains their radial position once formed [2]. Unlike the prompt splash drops on large plane surfaces that maintain a radial velocity allowing the motion away from the target, the receding breakup for small targets does not allow a radial velocity.

The three events (Deposition, Prompt splash and Receding corona breakup), follows three of six (Deposition, prompt splash, corona splash, receding breakup, partial and complete rebound), defined outcomes [2]. We did not observe the corona splash and two kinds of rebound under the examined experimental condition on a small target. Those events require surface beneath for initial spread to create the corona raise or complete receding for the rebound. Rebound on a small target was documented for a very short pillar with a hydrophobic coating. The drop continued the spreading along the lower surface [12]. Another bouncing received for a big drop-to-target ratio [13], with a close value to the impact non-dimensional maximal spreading diameter. Another drop response like drop-split requires a non-axisymmetric target or off-center drop impact [14] those cases are not discussed here. Each drop impact initiates with the drop free falling. Afterward, the drop spreads horizontally or coats the target. The drop shape becomes a film with a surrounding rim (Roisman, et al., 2002). The drop develops radial external fingers around the rim depending on the drop

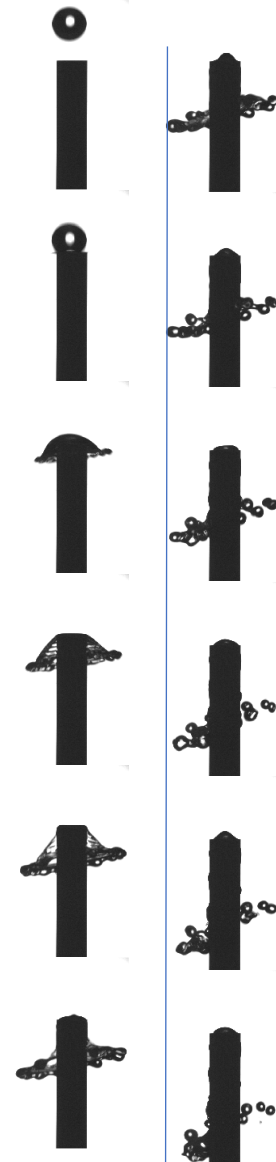


**Figure 4** Receding corona breakup, blue lines indicate the maximal spread.  $D_0 = 2.7[mm]$ ,  $D_t = 2.4[mm]$ ,  $v_0 = 1.6[m/s]$ , time sequences 1[ms]

stability. The growth of the lamella diameter, for example, reduces its stability. The number of the fingers and the diameter-length proportion indicate the drop's ability to remain united. The radial spread acceleration during the spreading controls the finger's length and number and affects the size distribution of secondary drops [15]. The differences between the drop responses stem from the initial conditions and the balance between the inertial forces and the internal forces, which are the viscosity and surface tension forces.

The drop spread time evolution demonstrates the after-events behavior. Figure 5 presents the events for a drop impact, which differ only by the initial velocity, as shown in Table 1. The deposition spread ends with receding at a similar pace as the spreading phase, and the other two events barely recede.

**Table 1** Experimental drop data for **Figure 5**

After-event	$D_0$ [mm]	$v_0$ [m/s]	$D_t$ [mm]	Material	Demonstrated
Deposition	2.7	1.65	2.4	Water	<b>Figure 1</b>
Breakup	2.7	1.9	2.4	Water	<b>Figure 4</b>
Splash	2.7	2.75	2.4	Water	<b>Figure 2</b>

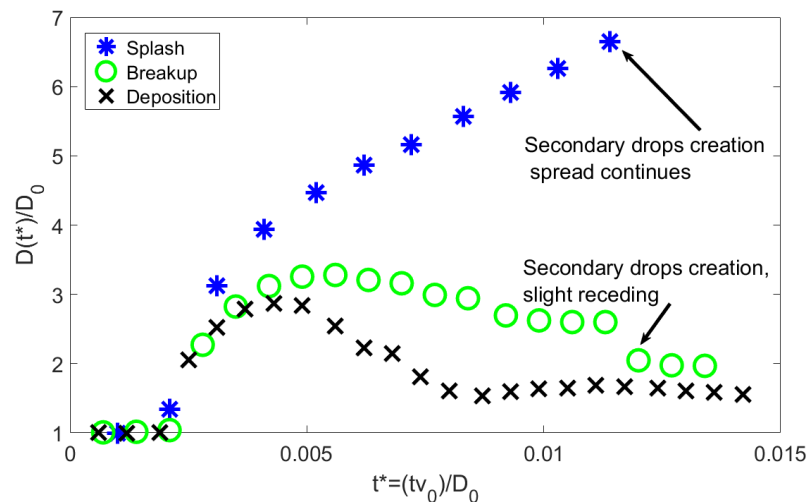


**Figure 5.** Drops spread evolution, dimensionless drop diameter as a function of the dimensionless time  $t^* = tv_0/D_0$ . Each curve represents a different impact after-event, with accordant to Table 1

## Conclusions

We observed the liquid drops in the different phases after impacting a small target and identified three primary after-events in response to the initial condition: prompt splash, receding corona breakup, and deposition; these outcomes results were received in this order respectively to the reduction in the initial velocity.

We did not observe the corona splash and two kinds of rebound under the examined experimental condition of a hydrophilic system and a small target. Those events require surface beneath for initial spread to create the corona raise or complete receding for the rebound.

The experiments performed in this study discussed three variants of the drop impact phenomenon by using different velocities and target diameters. Each velocity or diameter change modified the after-event for the same experimental conditions.

The developing lamella stability is affecting the response. We can deduce from the outcome that for the same drop diameter, the probability for a prompt splash increases by higher

velocity. Moreover, for the small target case, as the target diameter increases, the likelihood of breakup or splash increases.

Our previous study [8] shows that different target-to-drop diameter ratio has different spread patterns. Future research should characterize the effect of those patterns on the drop impact after-events by referring to the velocity effect as demonstrated in this study.

### Nomenclature

$D_0$	Drop initial diameter [mm]
$D(t^*)$	Drop diameter at time $t^*$ [mm]
$D_t$	Target diameter [mm]
$v_0$	Drop initial velocity [mm/msec]
$t^*$	Dimensionless time

### References

- [1] M. Rein, 1993, *Fluid Dynamics Research*, vol. 12, p. 61.
- [2] R. Rioboo, C. Tropea, and M. Marengo, 2001, vol. 11, no. 2, pp. 155–165.
- [3] Y. Hardalupas, A. M. K. P. Taylor, and J. H. Wilkins, 1999, *International Journal of Heat and Fluid Flow*, vol. 20, pp. 477–485.
- [4] S. Y. Yoon, H. Y. Kim, D. Lee, N. Kim, R. A. Jepsen, and S. C. James, 2009, *Drying Technology*, vol. 27, no. 2, pp. 258–266.
- [5] A. Rozhkov, B. Prunet-Foch, and M. Vignes-Adler, 2002, *Physics of Fluids*, vol. 14, no. 10, pp. 3485–3501.
- [6] G. Juarez, T. Gastopoulos, Y. Zhang, M. L. Siegel, and P. E. Arratia, 2012 *Physical Review E - Statistical, Nonlinear, and Soft Matter Physics*, vol. 85, no. 2.
- [7] R. Gupta, V. Vaikuntanathan, and D. Sivakumar, 2016, *Colloids and Surfaces A: Physicochemical and Engineering Aspects*, vol. 500, pp. 45–53.
- [8] M. Arogeti, E. Sher, and T. Bar-Kohany, 2019, *Chemical Engineering Science*, vol. 193, pp. 89–101.
- [9] E. Villermaux, 2007, *Annual Review of Fluid Mechanics*, vol. 39, pp. 419–446.
- [10] E. Villermaux and B. Bossa, 2011, *Journal of Fluid Mechanics*, vol. 668, pp. 412–435.
- [11] L. Yang, Z. Li, T. Yang, Y. Chi, and P. Zhang, 2021, *Langmuir*, vol. 37, no. 36, pp. 10838–10848.
- [12] S. Ding, Z. Hu, L. Dai, X. Zhang, and X. Wu, 2021 *Physics of Fluids*, vol. 33, no. 10, Oct. 2021.
- [13] S. Ding, X. Liu, X. Wu, and X. Zhang, 2020, *Physics of Fluids*, vol. 32, no. 10.
- [14] M. Arogeti, D. Sher, and E. Sher, 2018, *Experimental Thermal and Fluid Science*, vol. 99, pp. 140–148.
- [15] S. D. Aziz and S. Chandra, 2000, *International Journal of Heat and Mass Transfer*, vol. 43, pp. 2841–2857.